



Journal Name

ARTICLE

Electronic Supporting Information

Intercalation Pseudocapacitance in NASICON-Structured $\text{Na}_2\text{CrTi}(\text{PO}_4)_3$ @Carbon nanocomposite: Towards High-Rate and Long Lifespan Sodium-Ion-based Energy Storage

Dongxue Wang,^{‡a} Zhixuan Wei,^{‡a} Yunxiang Lin,^b Nan Chen,^a Yu Gao,^{*a} Gang Chen,^a Li Song,^b and Fei Du^{*a}

^aKey Laboratory of Physics and Technology for Advanced Batteries (Ministry of Education), State Key Laboratory of Superhard Materials, College of Physics, Jilin University, Changchun, 130012, People's Republic of China

^bNational Synchrotron Radiation Laboratory, CAS Center for Excellence in Nanoscience, University of Science and Technology of China, Hefei 230029, Anhui, People's Republic of China

*Corresponding authors.

E-mail addresses: dufei@jlu.edu.cn, yugao@jlu.edu.cn.

[‡]These authors contributed equally to this work.

Supplementary Figures

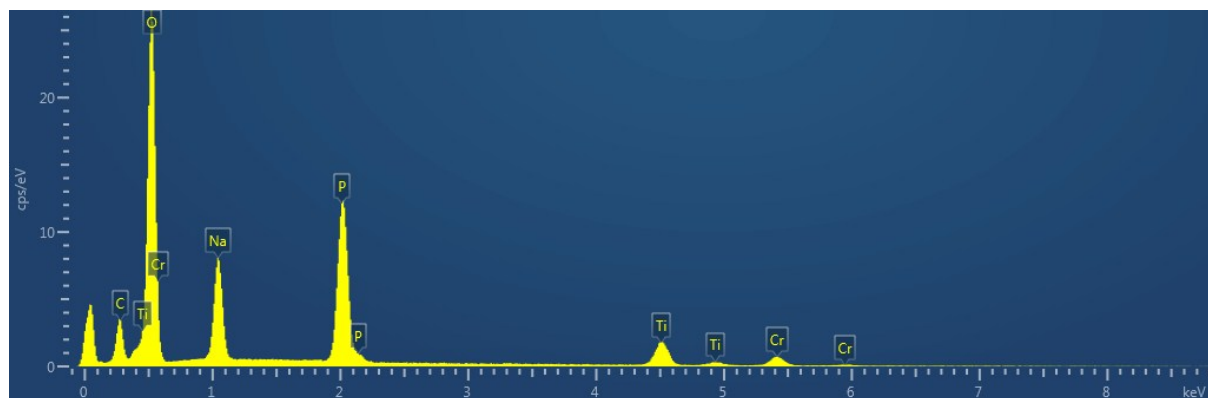


Figure S1. The EDX pattern of Na₂CrTi(PO₄)₃@C nanoparticles

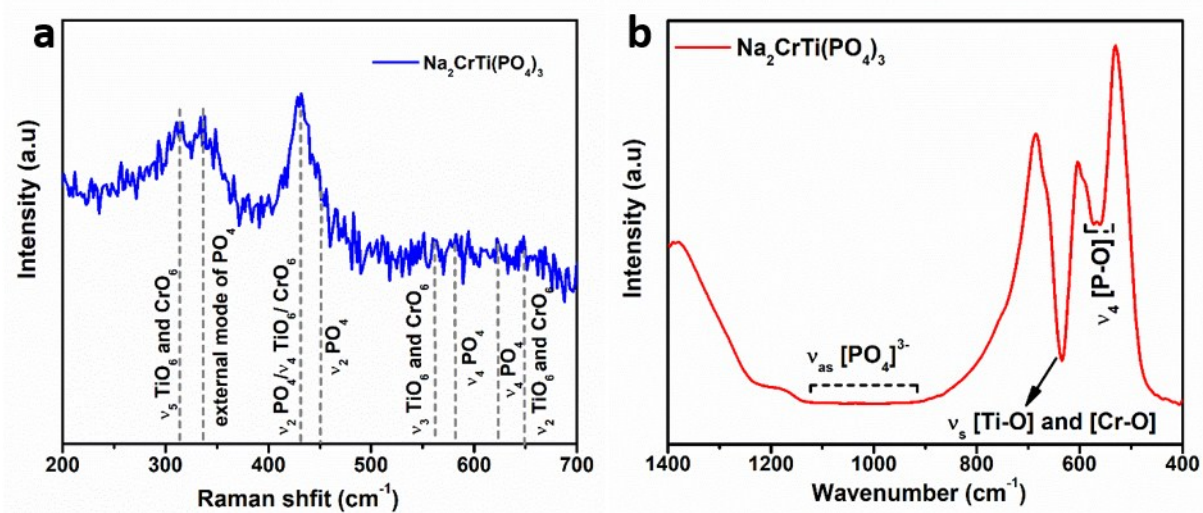


Figure S2. (a) Raman and (b) FT-IR spectrum of $\text{Na}_2\text{CrTi}(\text{PO}_4)_3$ @C nanoparticles

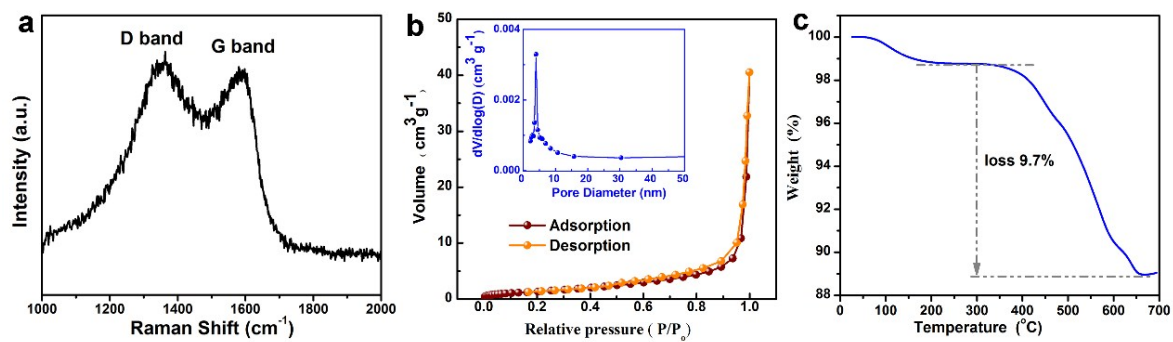


Figure S3. (a) Raman spectrum; (b) N₂ absorption–desorption isotherms with the pore-size distribution as the inset and (c) TG curve of Na₂CrTi(PO₄)₃@C nanoparticles.

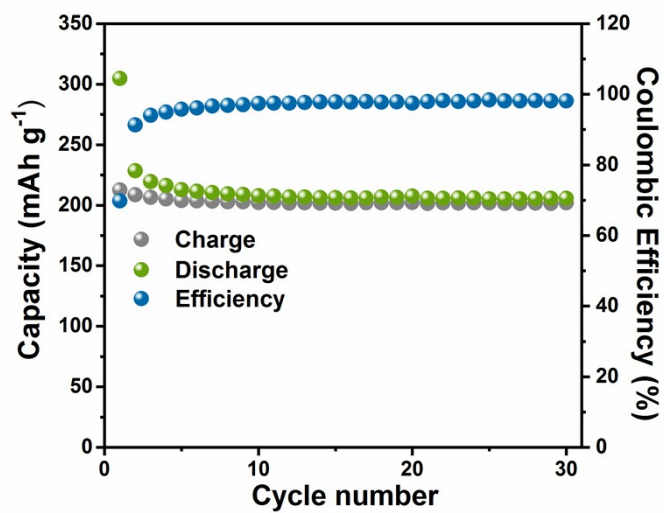


Figure S4. Cycle performance of $\text{Na}_2\text{CrTi}(\text{PO}_4)_3@C$ anode over 30 times under the current density of 20 mA g^{-1} .

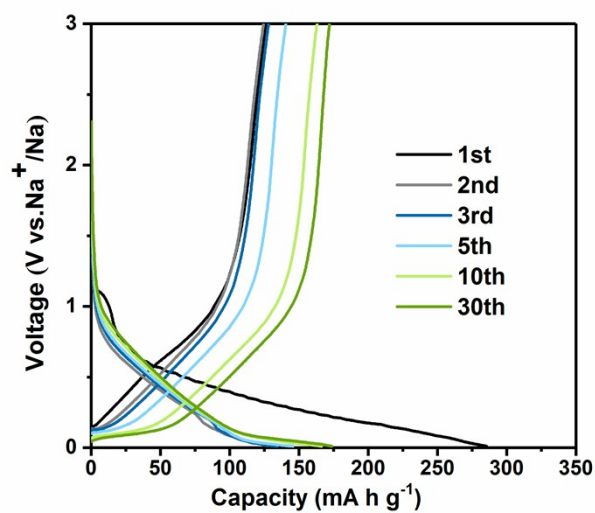


Figure S5. The 1st, 2nd, 3rd, 5th, 10th and 30th galvanostatic charge–discharge profiles of carbon at a current density of 20 mA g⁻¹.

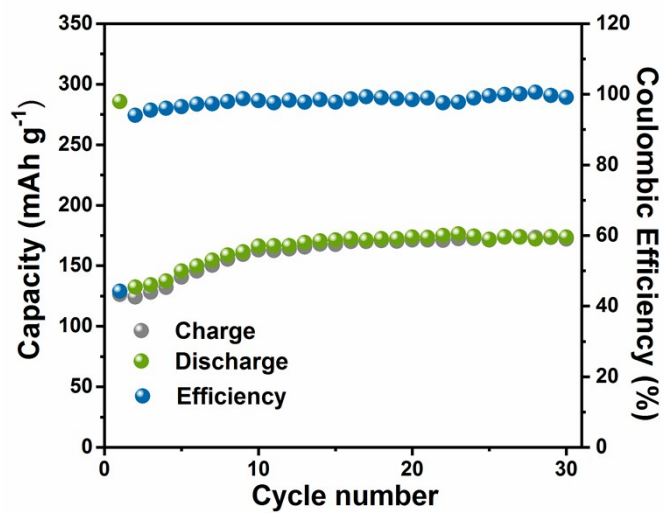


Figure S6. Cycle performance of carbon anode over 30 times under the current density of 20 mA g⁻¹.

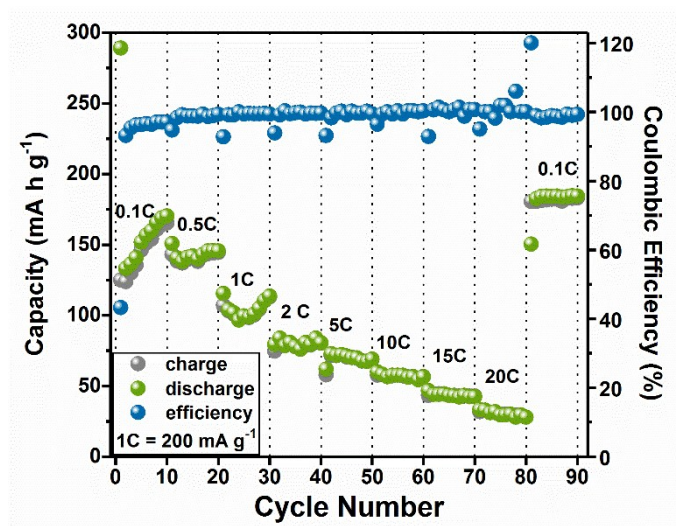


Figure S7. Rate performance of carbon.

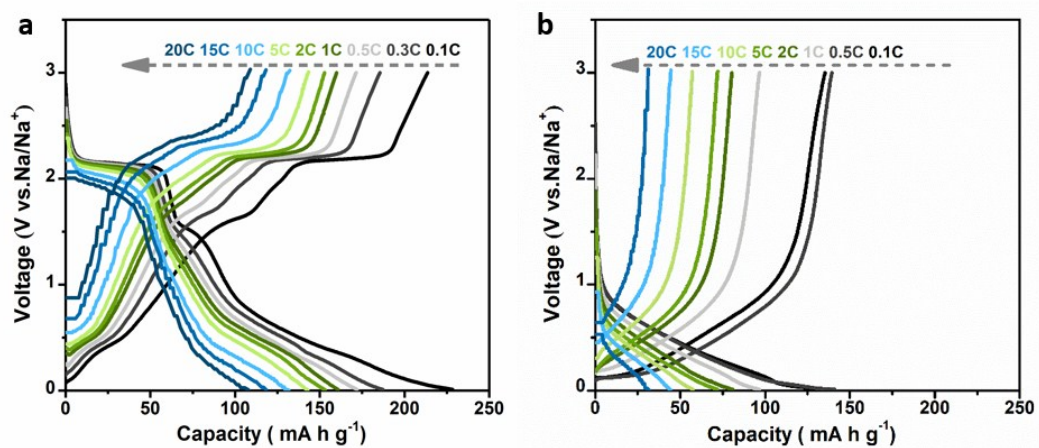


Figure S8. The galvanostatic charge-discharge curves of Na₂CrTi(PO₄)₃@C (a) and carbon (b) at different current densities

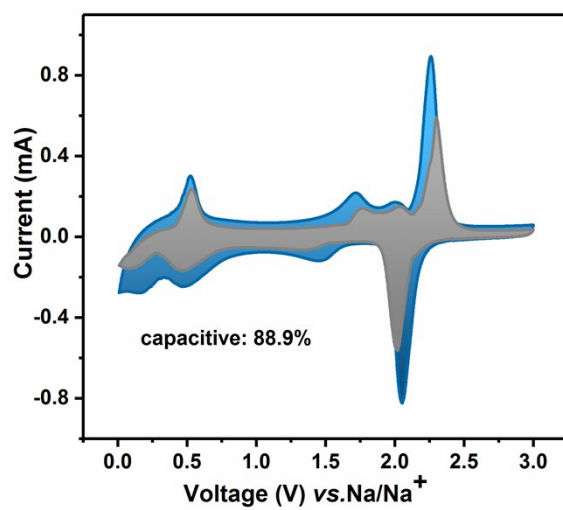


Figure S9. Separation of capacitive (shaded region) and diffusion-controlled contribution at 1 mV s^{-1} .

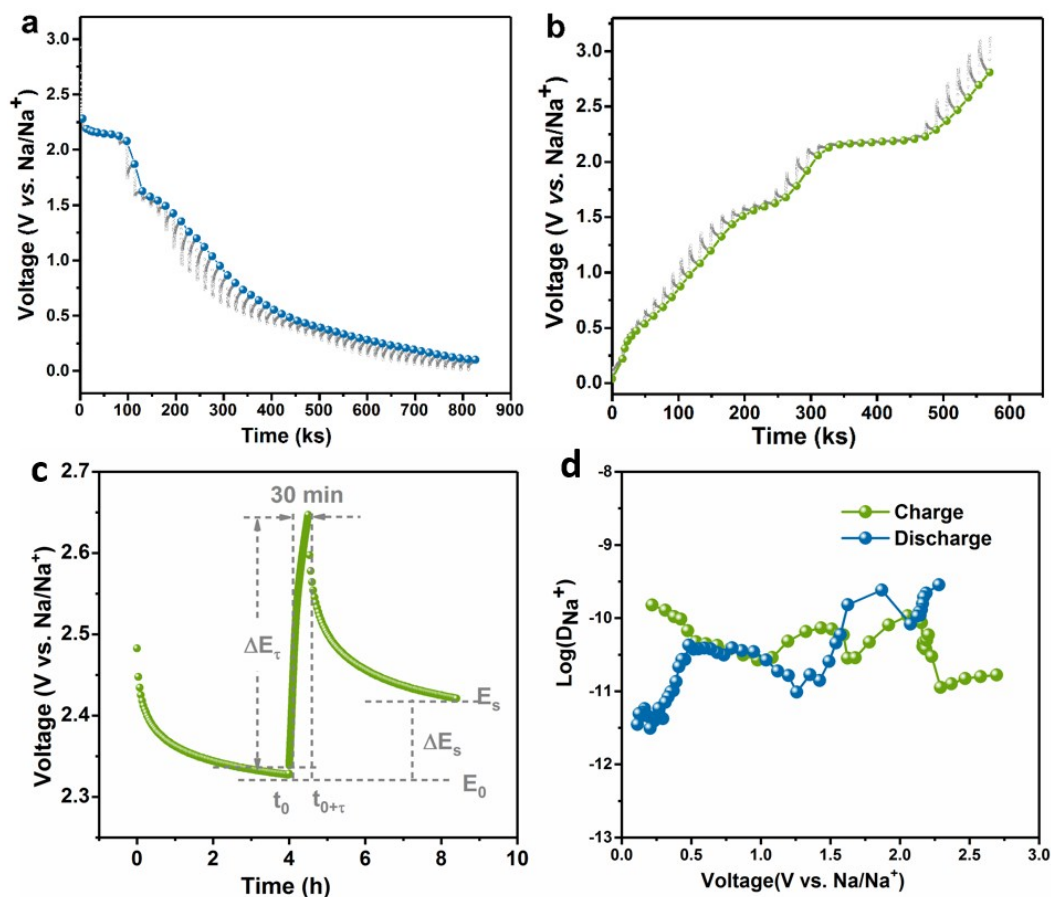


Figure S10. GITT profiles of $\text{Na}_2\text{CrTi}(\text{PO}_4)_3@\text{C}$ during the 2nd discharge (a) and charge (b) progress; (c) Current step diagram of $\text{Na}_2\text{CrTi}(\text{PO}_4)_3@\text{C}$ at 2.42 V vs. Na/Na^+ in the 2nd desodiation process (d) Diffusion coefficient calculated from GITT potential profiles.

The galvanostatic intermittent titration technique (GITT) was carried out in a coin cell after the initial cycle to evaluate the apparent diffusion coefficient (D_{Na^+}) for $\text{Na}_2\text{CrTi}(\text{PO}_4)_3@\text{C}$ nanoparticles. The quasi-equilibrium potentials for both initial sodiation (Figure S10a) and desodiation (Figure S10b) progresses are consistent well with the discharge-charge curves of $\text{Na}_2\text{CrTi}(\text{PO}_4)_3@\text{C}$ nanocomposites with little overpotential less than 0.38 V in both sodiation and desodiation progress, which indicated large ion diffusion coefficient of the (de)sodiation processes. The quantitative diffusion coefficient in $\text{Na}_2\text{CrTi}(\text{PO}_4)_3@\text{C}$ anode as a function of voltage is displayed in Figure S10d with detailed calculation method shown in Figure S10c. The GITT-determined diffusion coefficient is calculated as ranging from ca. 10^{-9} to 10^{-11} $\text{cm}^2 \text{ s}^{-1}$ during the 2nd discharge progress and the following charge progress, which is comparable to other NASICON-type compounds but higher than those compounds with layer structure. The higher D_{Na^+} of $\text{Na}_2\text{CrTi}(\text{PO}_4)_3@\text{C}$ can be ascribed to the 3D framework of $\text{Na}_2\text{CrTi}(\text{PO}_4)_3@\text{C}$ and the nano particle size as well as the high electronic conductivity contributed by the carbon complex.

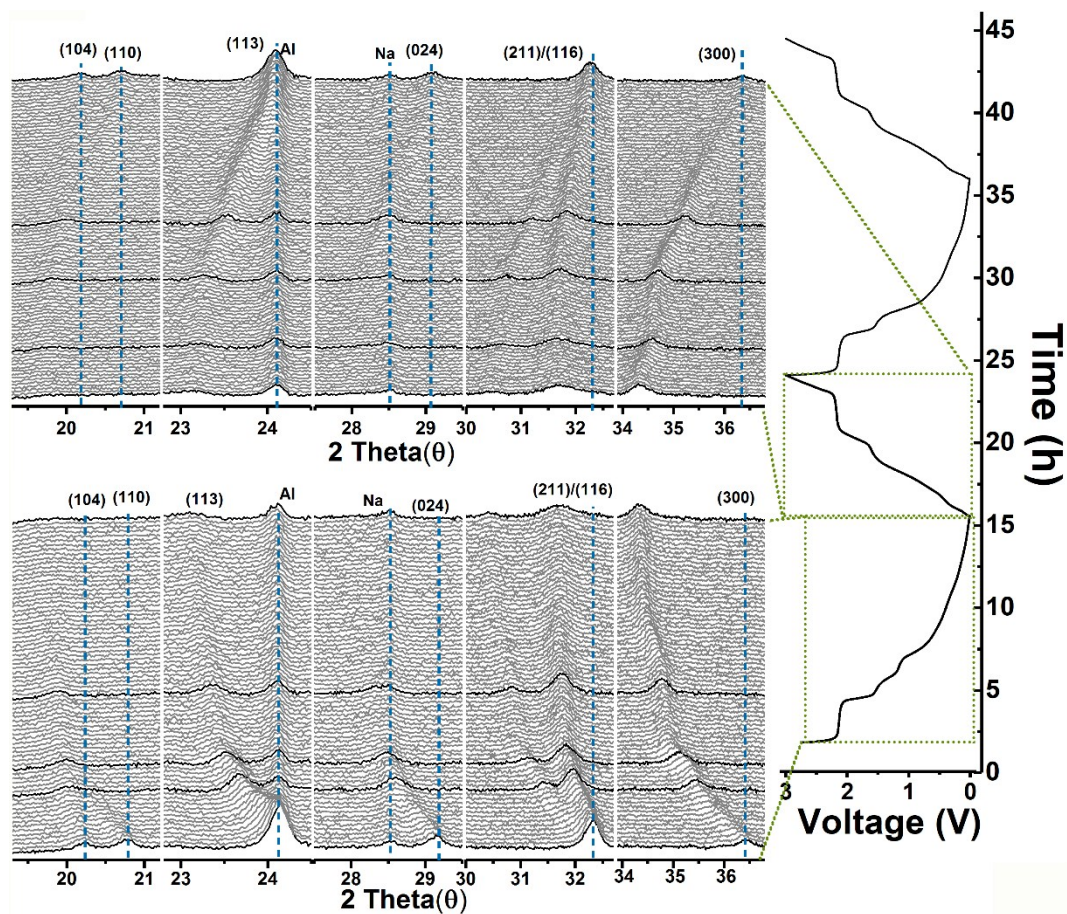


Figure S11. The enlarged in situ XRD patterns for the whole 1st discharge-charge progress with the corresponding discharge profiles on the right hand.

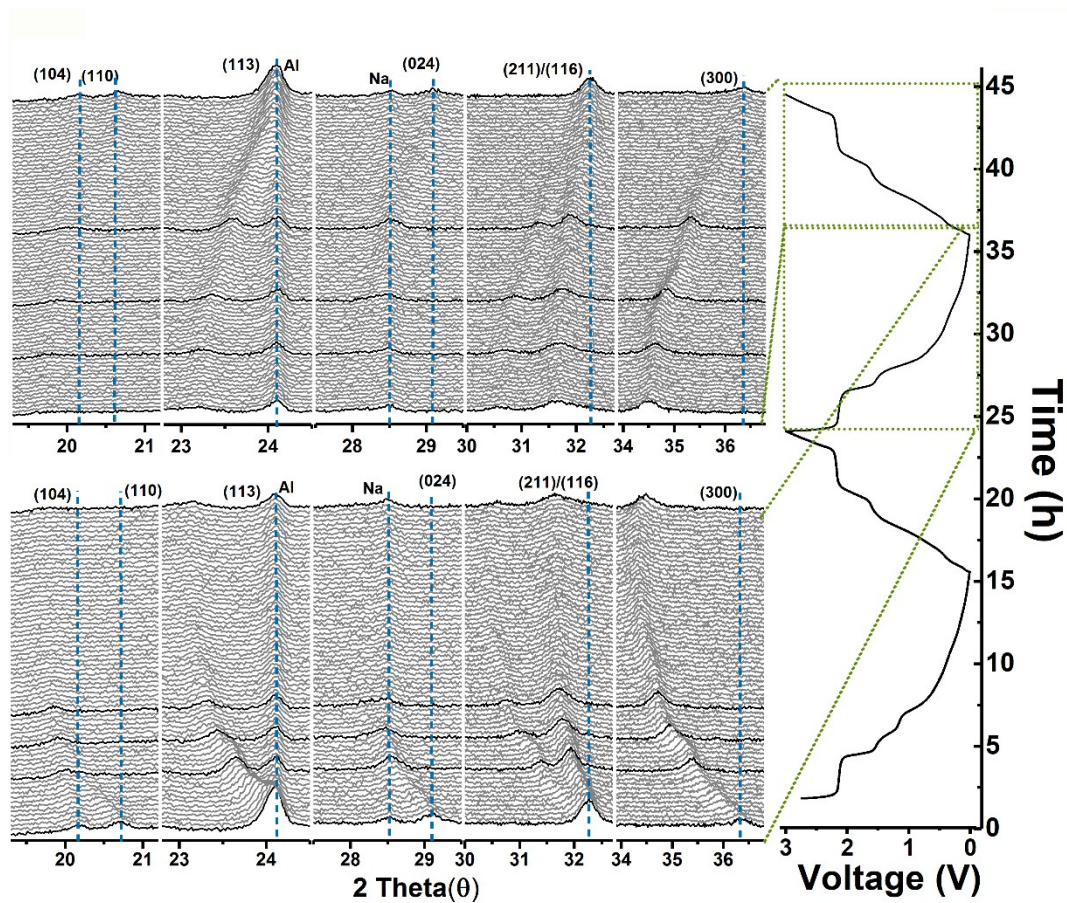


Figure S12. The enlarged in situ XRD patterns for the whole 2nd discharge-charge progress with the corresponding discharge profiles on the right hand.

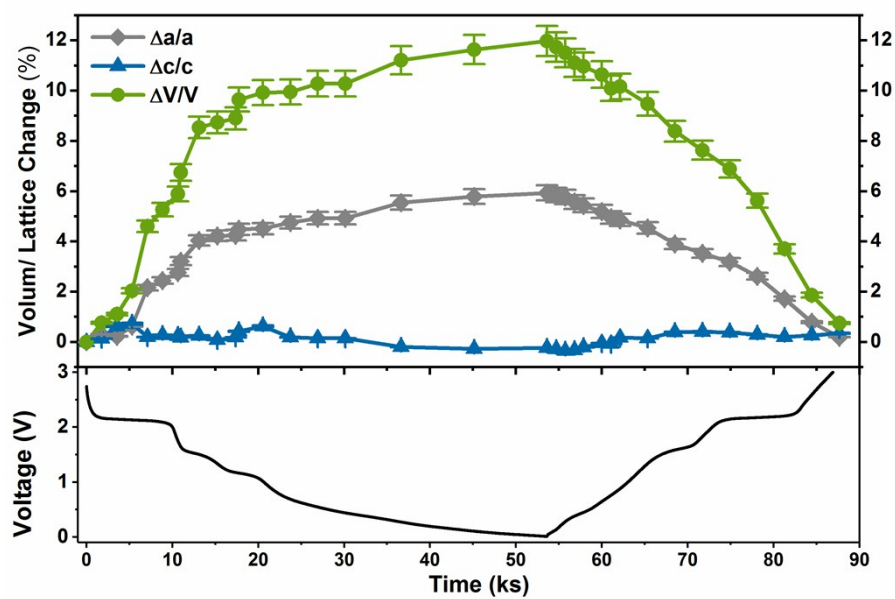


Figure S13. The evolution of lattice parameters during the initial cycle process.

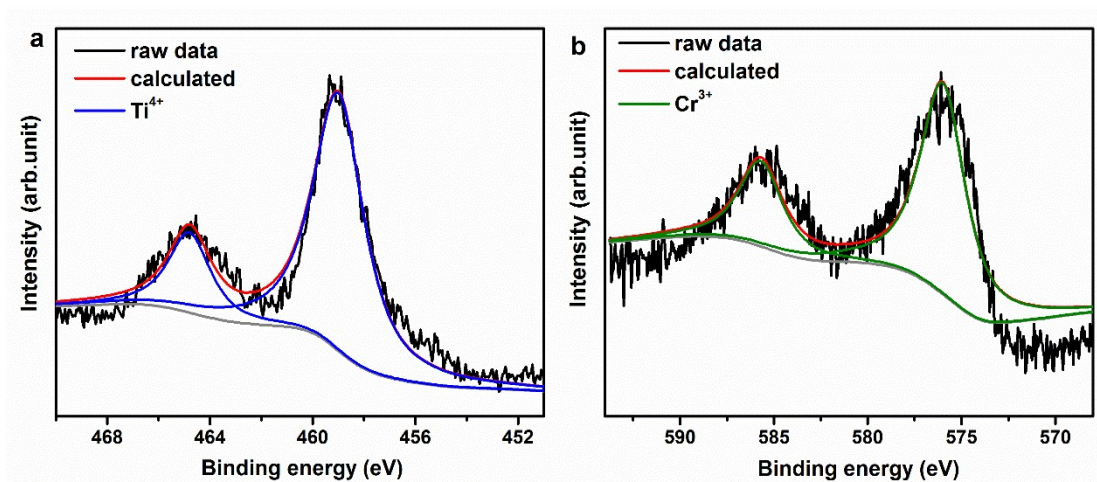


Figure S14. XPS spectrum of (a) Ti 2p and (b) Cr 2p in the Na₂CrTi(PO₄)₃@C electrode.

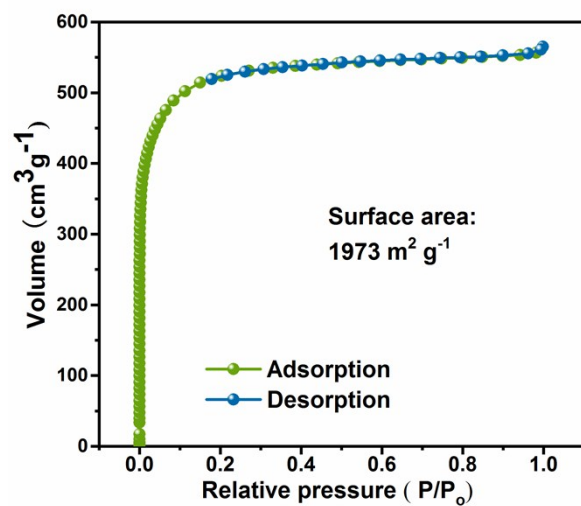


Figure S15. N₂ adsorption–desorption isotherms of AC.

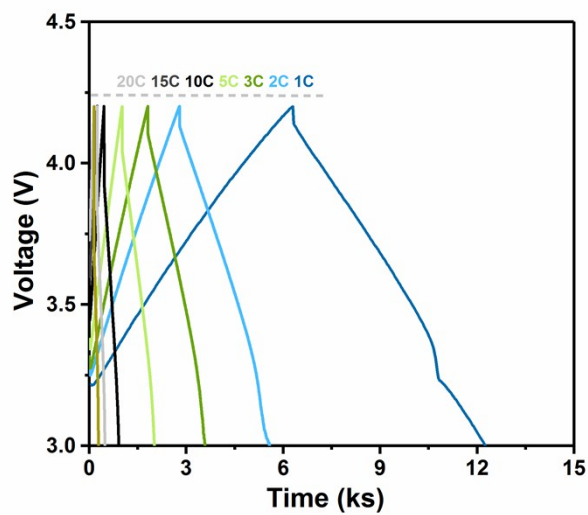


Figure S16. Profile of charge-discharge curves of [AC|| Na] capacitors at different current densities.

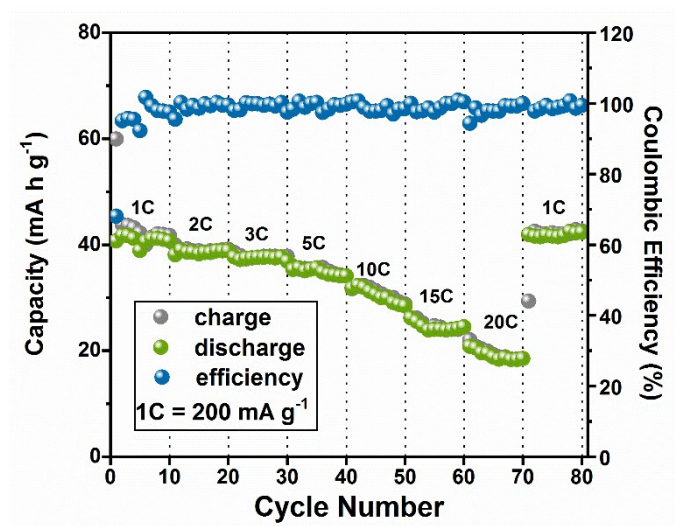


Figure S17. Rate performance of AC at different current densities.

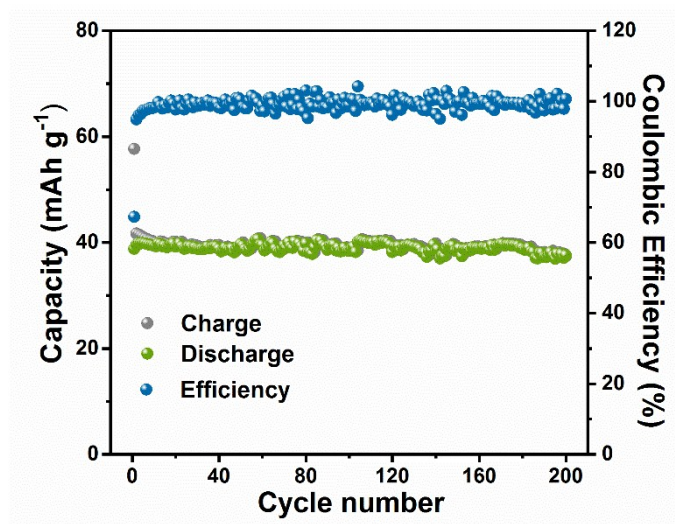


Figure S18. Cycle performance of AC over 200 times under the current density of 200 mA g⁻¹.

Supplementary Table 1. The atomic positions of Na₂CrTi(PO₄)₃@C nanocomposite upon Rietveld refinement results.

	Wyckoff position	x	y	z	Biso	Occ
Na1	<i>6b</i>	0	0	0	4.7477(8)	1.028(6)
Na2	<i>18e</i>	0.6350(5)	0	0.25	4.7477(8)	0.317(3)
Cr	<i>12c</i>	0	0	0.1462(9)	0.0397(3)	0.5
Ti	<i>12c</i>	0	0	0.1462(9)	0.0397(3)	0.5
P	<i>18e</i>	0.2894(2)	0	0.25	0.7051(0)	1
O1	<i>36f</i>	0.1919(5)	0.1667(1)	0.0883(7)	0.4153(8)	1
O2	<i>36f</i>	0.0273(5)	0.2036(5)	0.1929(7)	0.4153(8)	1

Space Group: *R-3c*, *a*=8.5440(8), *c*=21.7986(7), *R*_{wp}=11.6, *R*_p=8.93